Micropore Formation by Acid Treatment of Antigorite

K. Kosuge,*,† K. Shimada,‡ and A. Tsunashima†

National Institute for Resources and Environment, 16-3 Onogawa, Tsukuba 305, Japan, and Toho Olivine Industrial Co., Ltd., 3-4-2 Kyobashi Chuo-ku, Tokyo 104, Japan

Received June 15, 1995. Revised Manuscript Received September 7, 1995®

Microporous materials are prepared by H_2SO_4 treatment of antigorite ($Mg_3Si_2O_5(OH)_4$) and characterized mainly by SEM observation, a gas adsorption method, and ^{29}Si MAS NMR spectroscopy. The microtexture of the acid-treated products retains the morphology of the original ore composed of antigorite-like platy masses. Micropores 1 nm in size are formed between the layers of SiO_4-tetrahedron by Mg^{2+} dissolution. The micropore structure is changed by a condensation of silanol groups occurring in the pores. The maximum specific surface area is around 400 m^2/g, pore volume is 0.22 mL/g, and mean pore diameter is 1.2 nm. Around 5% MgO is necessary to stabilize the micropore structure and achieve a specific surface area of over 300 m^2/g. Mg^{2+} dissolution finally leads to formation of an amorphous silica with more than 99% SiO_2 content of which the specific surface area, pore volume and mean pore diameter are 170 m^2/g, 0.08 mL/g, and 2.0 nm, respectively.

Introduction

Acid treatment of silicates is a classical and common technique to obtain new and more useful products for industrial applications, such as adsorbents, catalysts, and catalyst carriers.[1-3] Dissolution of cations from a crystal framework generally leads to formation of an amorphous hydrated silica with complete breakdown of the original structure. However, acid treatment of some minerals is known to result in formation of a porous material with a texture similar to that of the original mineral.[4-6]

Antigorite ($Mg_3Si_2O_5(OH)_4$) is a magnesium hydrate silicate which is the main component mineral in serpentine. The ore exists in large quantities on the earth's surface including in Japan and many chemical processes which require use of magnesium had been investigated.[7-9] Serpentinite, however, has been rarely noted as a raw material for silica production. Girgis and Mourad[10] studied changes in textural parameters due to creation of micropores in antigorite by Mg^{2+} dissolution using only the adsorption isotherms of nitrogen. Recently, ^{27}Al and ^{29}Si magic angle spinning nuclear magnetic resonance (MAS NMR) spectroscopy has been widely used in both mineralogy and chemistry as a powerful probe of the static structure and dynamic behavior of condensed phases. The crystal structural changes of silicates with acid treatment have rarely been studied using an MAS NMR technique.[11,12]

In this research, H_2SO_4 of varying concentrations was used for treatment of samples for various reaction times to investigate the dependence of degree of Mg^{2+} dissolution on the microporous properties. The micropore structures were characterized in detail from gas adsorption data obtained using various types of molecules by BET analysis, *t*-plots, and fractal analysis. Furthermore, the micropore formation process was investigated by ^{29}Si MAS NMR spectral analysis and SEM observation as well as by analysis of the adsorption data.

Experimental Section

Materials. Serpentinite from Kouchi Prefecture, Japan, supplied by Toho Olivine Co., Ltd., was used as raw material. Antigorite used was a refined compound prepared from fractionated serpentinite by elimination of magnetic materials using a wet magnetic separator. Its chemical composition (wt %) was SiO_2, 41.88; MgO, 39.62; Fe_2O_3, 2.59; CaO, 1.14; Al_2O_3, 1.18; Cr_2O_3, 0.15; and ignition loss (mainly structural water in antigorite and brucite), 12.96. The impurities of brucite and chrysotile were detected by X-ray powder diffraction analysis and SEM observation. Their presence in small quantities was considered to have no significant effect on our experimental results.

Acid Treatment. The sample (20 g) was treated with H_2SO_4 (150 mL) of known concentration (3, 4, or 5 M) with stirring at 100 °C for a prescribed time. The flasks were connected to a water-cooled refrigerator in order to maintain a constant acid concentration. The acid-treated product was filtered, washed with deionized water until free of SO_4^{2-}, and dried at 50 °C for 2 days. The products were designated based on acid-treatment conditions such as 3 M and 5M-6 which correspond to the products treated with 3 M of H_2SO_4 and with 5 M of H_2SO_4 for 6 h, respectively.

Characterization. X-ray powder diffraction (XRD) data were obtained using a Rigaku RU300 diffractometer with Cu Kα radiation. Scanning electron microscopic (SEM) observa-

† National Institute for Resources and Environment.
‡ Toho Olivine Industrial Co., Ltd.
® Abstract published in *Advance ACS Abstracts,* October 15, 1995.

(1) Gonzales, L.; Ibarra, L.; Rodrigues, A.; Chamorro, C. *J. Colloid Interface Sci.* **1986**, *109*, 150–160.
(2) Corma, A.; Perez-Pariente, J. *Clay Miner.* **1987**, *22*, 423–433.
(3) Rhodes, C. N.; Franks, G. M. B.; Brown, D. R. *J. Chem. Soc., Chem. Commun.* **1991**, 805–807.
(4) Frondel, C. *Am. Mineral.* **1979**, *64*, 799–804.
(5) Mendioroz, S.; Pajares, J. A.; Benito, I.; Pesquera, C.; Gonzales, F.; Blanco, C. *Langmuir* **1987**, *3*, 676–681.
(6) Jovanovic, N.; Janackovic J. *Appl. Clay Sci.* **1991**, *6*, 59–68.
(7) Arai, Y.; Nagai, S. *Kagaku to Kogyo* **1963**, *16*, 23–32.
(8) Mase, H. *Kogyo Kagaku Zasshi* **1955**, *58*, 92–95.
(9) Petrovski, P.; Gligoric, M.; Nisevic, M.; Begagic, M. *High Tech Ceramics*; Vincenzini, Ed.; Elsevier Science Publishers B.V.: Amsterdam, 1987 pp 2267–2278.
(10) Girgis, B. S.; Mourad, W. E. *J. Appl. Chem. Biotechnol.* **1976**, *26*, 9–14.
(11) Tkac, I.; Komadel, P.; Muller, D. *Clay Miner.* **1994**, *29*, 11–19.
(12) Kaviratna, H.; Pinnavaia, T. J. *Clays Clay Miner.* **1994**, *42*, 717–723.

0897-4756/95/2807-2241$09.00/0

Table 1. Microporous Parameters of the Acid-Treated Products[a]

concn (M)	reaction time (h)	MgO (%)	microporous parameter S_{BET} (m^2/g)	S_{int} (m^2/g)	V (mL/g)	$2t$ (nm)	fractal dimension D
3	2	24.6	206	187	0.10	1.0	
	4	17.8	278	251	0.13	1.0	
	6	15.1	300	271	0.15	1.1	3.0
	8	12.6	313	284	0.16	1.1	
	18	4.9	389	354	0.20	1.1	2.9
	24	2.0	406	360	0.22	1.2	2.9
4	2	18.1	262	249	0.15	1.2	
	4	11.5	326	311	0.19	1.2	
	6	8.3	330	310	0.20	1.3	3.0
	8	3.3	360	337	0.23	1.4	
	18	2.1	332	303	0.22	1.4	2.6
	24	1.3	294	263	0.20	1.6	2.5
5	1	15.5	266	255	0.16	1.2	
	4	4.6	336	315	0.22	1.4	
	8	1.1	275	241	0.20	1.6	
	24	0.2	167	78	0.08	2.0	1.9

[a] S_{BET}, S_{int}, V, and $2t$ represent BET surface area, internal surface area, pore volume, and mean pore diameter, respectively. These values are determined by t-plot method. The D value is the surface fractal dimension for the BET monolayer adsorption, and found in the range of $2 \leq D < 3$ in nature.[14] The value provides information on the structure of the micropore wall. The D value near 3 indicates that the adsorbate molecules are of a scale similar to the roughness of the pore surface. Low $D = 2.0$ value indicates an ordered two-dimensional micropore wall.

tion was performed using a JEOL scanning electron microscope (JSM5300) and a conventional sample preparation method. The magnesium content in each product was determined by X-ray fluorescence (XRF) analysis with a Rigaku 300 spectrophotometer, after fusing a 0.5 g sample in 5 g of dilithium tetraborate using a beam-bed sampler at around 1200 °C. Thermogravimetric-differential thermal analysis (TG-DTA) was carried out with a Rigaku thermometer using a 5−6 mg sample at a heating rate of 15 °C/min.

Nitrogen adsorption−desorption isotherms were obtained at −196 °C on a computer-controlled volumetric BELSORP28. The isotherms of H_2O, CH_3OH, C_6H_6, and n-C_4H_{10} were obtained at 25 °C using a BELSORP18. Before the actual adsorption measurements, about 0.2 g of sample was heated in vacuo at 150 °C for 2 h, and finally outgassed at 10^{-3} Torr at room temperature. BET and t-plot analyses were used to determine the total specific surface area, internal specific surface area, mean pore diameter, and pore volume of the products.[13] Fractal analysis was applied to obtain information on the geometrical heterogeneity of the solid surface on a molecular scale.[14,15]

The ^{29}Si MAS NMR experiments were performed on a Brucker 200 MHz solid state NMR spectrometer at 39.64 MHz. Sample spinning frequency was in the range 4−4.2 kHz. Proton decoupling during acquisition was used. For cross-polarization (CP) MAS ^{29}Si NMR analysis the recycling delay time was 5 s and the number of scans was 1042 for each spectrum. Chemical shifts are referenced relative to TMS (tetramethylsilane).

Results and Discussion

Bulk Properties. Table 1 lists the MgO content of all acid-treated products in this work. Results of SEM observation as shown in Figure 1 revealed no morphological change of the products with acid treatment; i.e., after leaching the products retain platy masses of

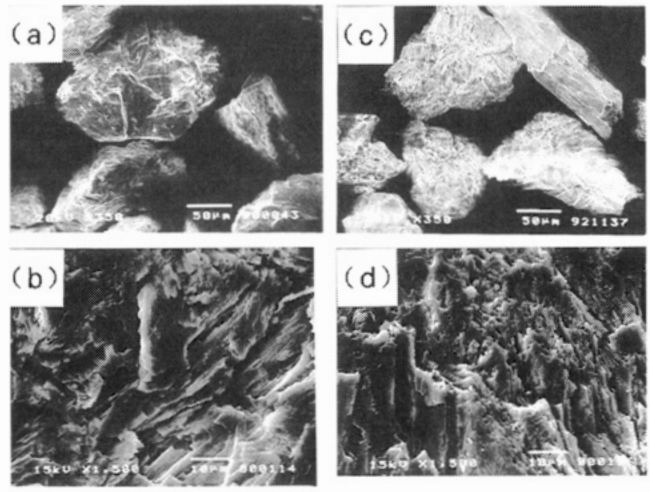

Figure 1. SEM micrographs of (a) and (b) untreated antigorite, and (c) and (d) 5M-24.

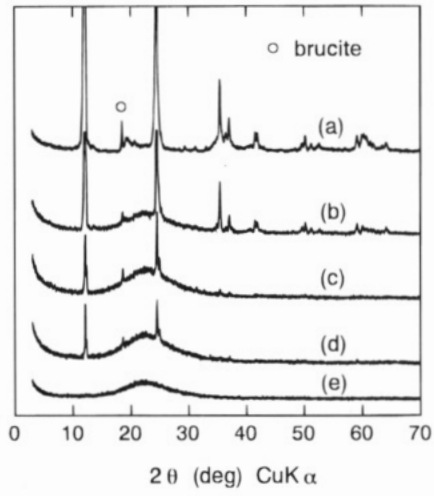

Figure 2. XRD patterns of (a) untreated antigorite, (b) 3M-6, (c) 3M-24, (d) 4M-24, and (e) 5M-24.

antigorite (Figure 1b,d). Representative XRD patterns of untreated antigorite and the acid-treated products are shown in Figure 2. The pattern for 5M-24 exhibits only one broad peak around 22.5° corresponding to an amorphous silica phase formed upon Mg^{2+} dissolution, while those of the other products show peaks, indicating the presence of antigorite as well as amorphous silica. Since the Si solubility was below 0.2% even in the case of 5M-24 and no precipitate on the solid surfaces was observed in the SEM micrograph (Figure 1d), the textural changes in this study are attributed only to Mg^{2+} dissolution.

TG-DTA curves of each acid-treated product showed a decrease in weight occurring at around 70 °C with an endothermic peak. Furthermore, the curves of 5M-18 and 5M-24 clearly showed a gradual decrease in weight occurring from 150 to 1000 °C. This decrease in weight not observed in the untreated ore is attributed to the evaporation of water contained in the amorphous silica as will be discussed later, and water content increased with increasing H_2SO_4 concentration and reaction time. It is possible to obtain amorphous silica with >99% SiO_2 content, if the ignition loss is excluded, from antigorite treated with 5M H_2SO_4 for more than 18 h.

Porous Properties. Representative adsorption−desorption isotherms of N_2 are shown in Figure 3. The

(13) de Boer, J. H.; Lippens, B. C.; Linsen, B. G.; Broekhoff, J. C. P.; van den Heuvel, A.; Osinga, Th. J. *J. Colloid Interface Sci.* **1966**, *21*, 405−414.
(14) Avnir, D.; Farin, D.; Pfeifer, P. *Nature* **1984**, *308*, 261−263.
(15) Ishikawa, T.; Kodaira, N.; Kandori, K. *J. Chem. Soc., Faraday Trans.* **1992**, *88*, 719−722.

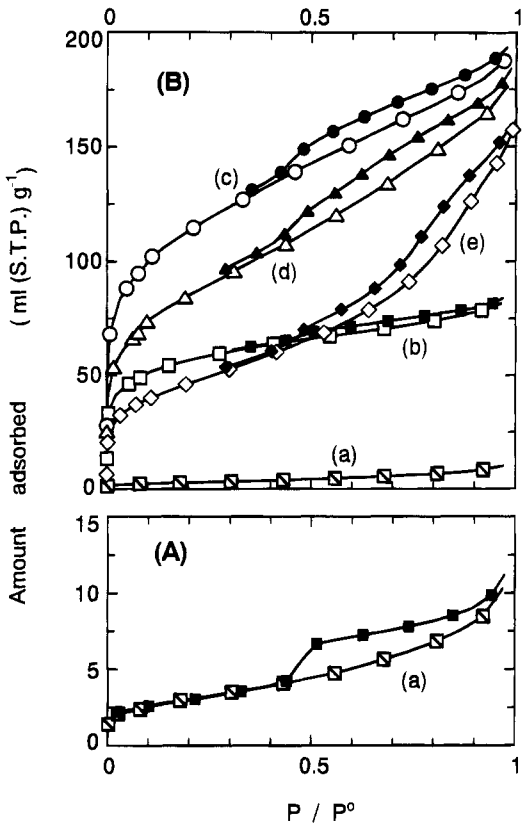

Figure 3. Nitrogen adsorption–desorption isotherms of (a) untreated antigorite, (b) 3M-2, (c) 3M-24, (d) 4M-24, and (e) 5M-24. (A) is for untreated antigorite. Open and closed symbols represent adsorption and desorption isotherms, respectively.

isotherms can be classified based on the BDDT (Burunauer, Deming, Deming, and Teller) classification.[16] Untreated antigorite shows isotherm of type **IV** (Figure 3A), and the isotherms of all acid-treated products are a mixture of types **I** and **IV** (Figure 3B). The hysteresis loop of the isotherm for untreated antigorite (Figure 3A) reveals the presence of mesopores such as slit-shaped pores bounded by parallel plates.[16] This type of mesopore is consistent with the interface morphology of platy crystals as observed by SEM (Figure 1b). Hysteresis loops were also observed in the N_2 adsorption–desorption isotherms of all acid-treated products and were attributed to effects of capillary condensation of N_2 into mesopores. An increase in the degree of Mg^{2+} dissolution leads to enlargement and broadening of the loop as shown in Figure 3 b–e. The present results on variation in shape of the loop suggest that aggregates of platy-like particles become increasingly loosely packed with increasing reaction time.

BET analysis of the adsorption isotherms shows that the BET surface area (S_{BET}) of the acid-treated products depends strongly on the acid treatment conditions (Table 1). S_{BET} for the untreated antigorite was about 5 m^2/g, and increased by a maximum of about 80-fold in the product upon Mg^{2+} dissolution. *t*-plot analysis is a useful method to evaluate from adsorption data microporous parameters such as internal specific surface area (S_{int}), mean pore diameter ($2t$), and pore volume (V).[13] The *t* curves for the corresponding

(16) Sing, K. S. W.; Everett, D. H.; Haul, R. A. W.; Moscou, L.; Pierotti, R. A.; Rouquerol, J.; Siemienewska, T. *Pure Appl. Chem.* **1985**, *57*, 603–619.

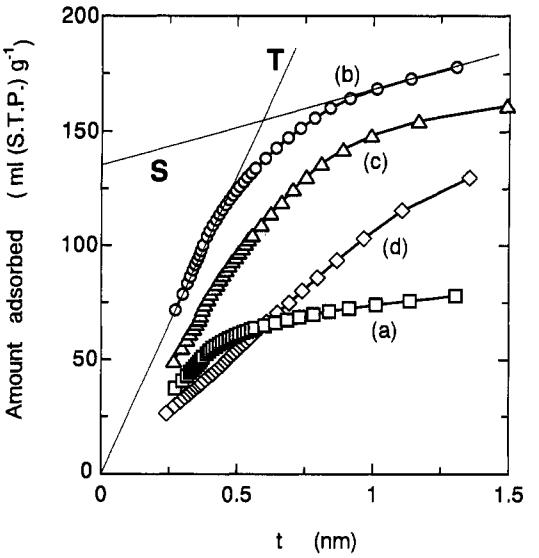

Figure 4. *t*-plots of (a) 3M-2, (b) 3M-24, (c) 4M-24, and (d) 5M-24. The intersection of the two straight lines of S and T corresponds to the mean pore diameter ($2t$).

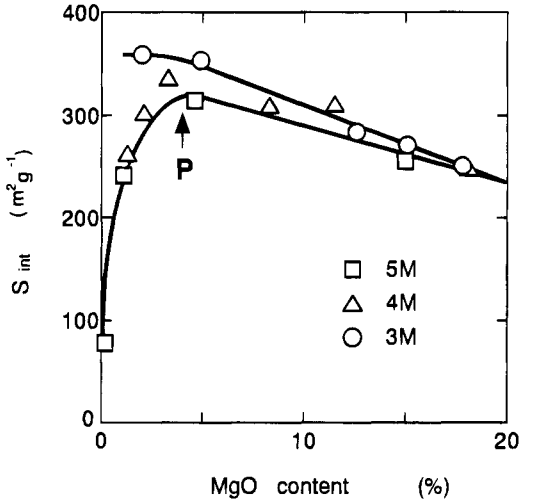

Figure 5. Relationship between MgO content and S_{int} of the acid-treated products. P represents the initiation point of the condensation of silanol groups created in the pores.

products in Figure 3 are shown in Figure 4. In the early stage of adsorption, *t* curves for all acid-treated products prepared in this work fit well the straight lines passing through the origin such as line T in Figure 4. The type of pore present can be determined from the deviation pattern of the *t* curve from the straight line as mentioned above. As shown in Figure 4, the *t* curves exhibit a downward deviation due to micropore filling, which reflects the type **I** isotherms.[13] The intersection of the two straight lines, one of which is obtained by interpolating the curve from $t > 1$ to $t = 0$ and the other of which is the line passing through the origin as noted by S and T in Figure 4, corresponds to the mean pore diameter ($2t$). V and S_{int}, respectively, refer to the cumulative volume and the specific surface area of pores smaller than the size represented by the intersection point. Table 1 lists values obtained for microporous parameters including S_{BET}, S_{int}, V, and $2t$ of the acid-treated products.

Figure 5 shows the relationship between MgO content and S_{int}. The proportion of S_{int} to S_{BET} is found to be more than 90% for almost all acid-treated products. In

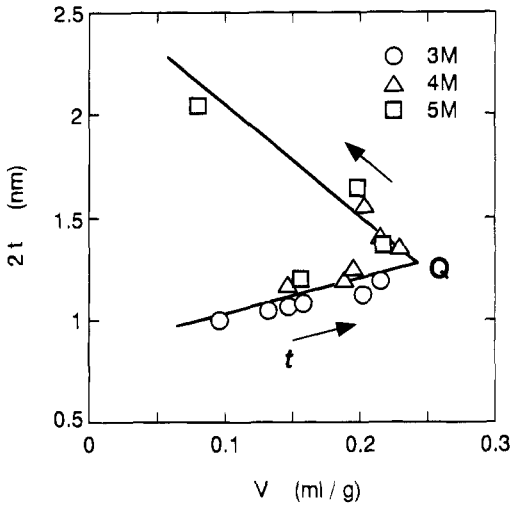

Figure 6. Relationship between V and $2t$ of the acid-treated products. Point Q represents the same point as that of point P in Figure 5.

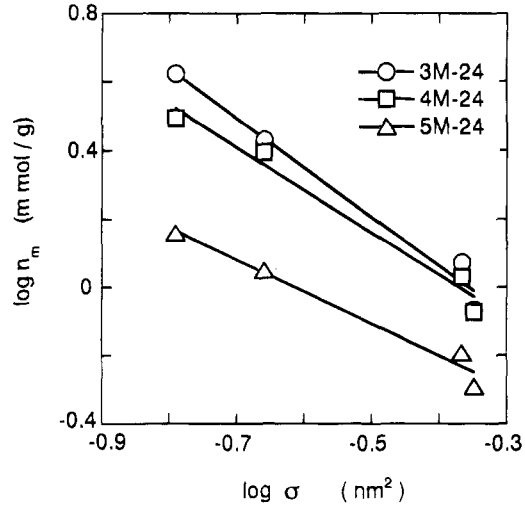

Figure 7. BET monolayer adsorption capacity, n_m, as a function of adsorbate cross section σ.

the case of 3 M H_2SO_4, S_{int} continued to increase up to 24 h of reaction time. However, the products turned brown due to formation of a colloidal precipitate on the solid surface by the hydration of soluble ions such as Fe^{3+}. On the other hand, the products showed increasing whiteness with increasing dissolution time using higher H_2SO_4 concentrations (4 and 5 M). S_{int}, however, reaches a maximum value (point P) at around 4.5% MgO and thereafter exhibits a steep decrease with small decrease in MgO content. These results indicate that the presence of a small amount of MgO in the acid-treated product is necessary to maintain micropore stability.

The variation in S_{int} indicates the structural change of micropores. To investigate this variation in S_{int}, the relationship between V and $2t$ of the products is shown in Figure 6 as a function of the duration of acid treatment represented by the arrows. Micropores around 1 nm in size were created at an early stage of acid treatment and $2t$ increases slightly with increasing V as the duration of acid treatment increases. From point Q, $2t$ increases markedly with decreasing V. The surface of acid-treated solid contains silanol groups.[1,11,12] Furthermore, the higher the acid concentration, the more reactive silanol groups are converted to siloxane groups by dehydration and condensation. It is evident from the above results that the formation of micropores is allowed to continue and the resulting pores exist stable irrespective of the acid concentration and the degree of Mg^{2+} dissolution until point Q in Figure 6. From point Q, the destruction of micropores is considered to begin by dehydration and condensation of silanol groups created in the pores.

Fractal Analysis of Micropores. Gas adsorption isotherms including those of N_2, C_6H_6, CH_3OH, and 1-C_4H_{10} were measured to investigate the properties of micropores in acid-treated products. Fractal analysis was carried out using the adsorption data and the following equation for estimating surface heterogeneity of solids:[14,15]

$$\log n_m = -(D/2)\log \sigma + C$$

where n_m, D, σ, and C are BET monolayer adsorption capacity, surface fractal dimension, cross-sectional area of adsorbed molecules, and a constant, respectively. The slope of this straight line gives the fractal dimension. Figure 7 shows the representative plots of log n_m vs log σ for the adsorbed molecules, indicating a good linear relationship. All D values obtained in this work are listed in Table 1, which shows that the D values range from 3 to 2. On the basis of the fractal dimension of $2 \leq D < 3$ reported for most materials,[14] the surfaces of the acid-treated products in this study were concluded to be fractals. While D values remain at around 3 in the case of 3 M H_2SO_4, a decrease in D value to less than 3 is caused by some degree of Mg^{2+} dissolution in the case of higher H_2SO_4 concentrations (4, 5 M), as shown in Table 1. Therefore, the fractal analysis results support the conclusion that the surfaces of the micropores that formed at an early stage of acid treatment and did not undergo destruction exhibited a D value of 3 due to their extreme irregularity. Furthermore, the point of change in D from 3 to a lower value is presumed to be the point of initiation of destruction of the micropores, represented by point P in Figure 5 and point Q in Figure 6.

Structural Change of Framework. The ^{29}Si MAS NMR spectra of the samples are shown in Figure 8A. The chemical shift of untreated antigorite is at −93.11 ppm for Q^3 units corresponding to a phyllosilicate, which is consistent with previously reported values.[17] The chemical shifts of the acid-treated products were assigned on the basis of published data[18,19] and the measured ^{29}Si spectra obtained by CP MAS NMR spectroscopy as shown in Figure 8B.

The downfield shift in the Q^3 unit from −93.11 to −90 ppm is the only change in the chemical shifts as shown in Figure 8A. To investigate this movement upon acid treatment, a comparison of the Q^3 unit of antigorite with that of chrysotile is not only informative but also pertinent, because chrysotile is a serpentine mineral and has almost the same chemical composition as

(17) Nakata, S.; Asaoka, S.; Kondo, T.; Takahashi, H. *Nendo Kagaku* **1986**, *26*, 197−208.
(18) Fyfe, C. A.; Gobbi, G. C.; Kennedy, G. J. *J. Phys. Chem.* **1985**, *89*, 277−281.
(19) Engelhardt, G.; Michel, D. *High-Resolution Solid-State NMR of Silicates and Zeolites*; J. Wiley: Chichester, 1987; p 154.

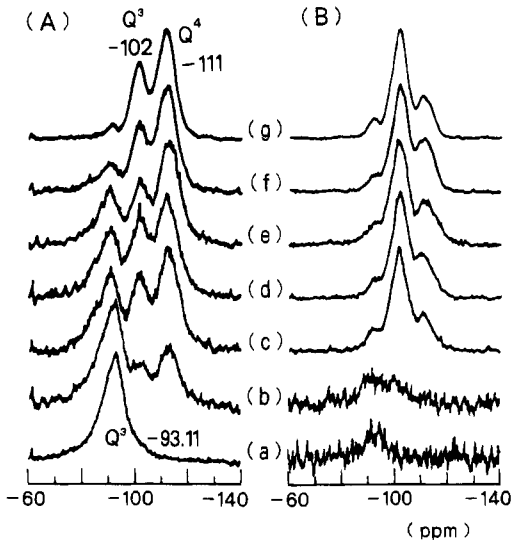

Figure 8. ^{29}Si MAS NMR spectra (A) and the CP MAS NMR spectra (B) of (a) untreated antigorite, (b) 3M-0, (c) 3M-0.5, (d) 3M-1, (e) 3M-2, (f) 3M-6, and (g) 5M-24.

antigorite. Even if Mg^{2+} was completely dissolved from the framework of chrysotile, little shift was observed in the chemical shift at −92.7 ppm for the Q^3 unit (unpublished data). The b_{oct} (the lattice parameter of an unstrained MgO_6 octahedral layer) value is only slightly smaller than the b_{tetr} (the lattice parameter of an unstrained hexagonal Si_2O_5 tetrahedral layer) value in serpentine minerals.[20,21] To reduce the stacking strain based on the misfit between the composite layers, antigorite has corrugated layers with periodical inversion of the SiO_4 tetrahedra as shown in Figure 9a, and the layers in chrysotile are rolled up like a carpet.[20,21] Mg^{2+} dissolution would result in a structural change of the residual framework or Si_2O_5-tetrahedral layer by reduction of the stacking strain. However, since Q^2 units were not observed in the spectra of all acid-treated products, we concluded that Si_2O_5 sheets were not fragmented even in the case of amorphous silica with low MgO content. This agrees with an absence of morphological change before and after acid treatment of antigorite observed in SEM micrographs (Figure 1). Hence, we believe that the flattening of the layers as shown in Figure 9b would occur in antigorite upon Mg^{2+} dissolution but not in chrysotile due to the higher degree of curvature of the composite layers. The established correlations demonstrate unambiguously that the ^{29}Si chemical shift depends sensitively on the mean bond length of SiO (d_{SiO}) and Si−O−Si bond angle (α), with downfield shifts at greater d_{SiO} and at smaller α value.[22,23] The decrease in α of antigorite may arise from the flattening of the layers, consistent with the downfield shift of Q^3 unit as mentioned above.

Micropore Formation. On the basis of the NMR data, adsorption data and results of morphological observation, a possible process of formation and transformation of micropores upon acid treatment of antigorite is proposed and schematically summarized in Figure 9. However, these schematics can illustrate textural changes within a very limited region and never throughout the bulk.

With the dissolution of the octahedral layers new surfaces appear facing each other as shown in Figure 9b. These surfaces are expected to carry silanol groups and be very reactive, i.e., highly susceptible to condensation induced by sliding of adjacent silicate layers. The sliding and subsequent direct interconnection of the silicate layers results in creation of micropores containing water molecules between the layers as shown in Figure 9c. The weight loss occurring at less than 100 °C detected by TG-DTA as mentioned before is attributed to the evaporation of water from the micropores. Taking into account the lattice parameters of antigorite,[21] the pore size of around 1 nm can be explained by assuming the dissolution of three successive MgO_6-octahedral layers (Figure 9b,c). Part A in Figure 9b gives the chemical shift at −102 ppm for Q^3 ($(SiO)_3SiOH$) as shown in Figure 8, indicating that Si atoms bearing OH groups are formed upon acid treatment, because a strong signal corresponding to this shift is observed in the CP MAS ^{29}Si NMR spectrum (Figure 8B). Furthermore, part B in the same figure gives the chemical shift at −111 ppm for Q^4 ($(SiO)_4Si$) as shown in Figure 8. As a result of condensation of the hydroxy groups and formation of siloxane bonds, part B with a three-dimensional cross-linked framework is formed. The dependence of the integral intensities for individual structural units in leached products on the duration of acid treatment is presented in Figure 10. The intensities for each unit increase/decrease significantly until 6 h and thereafter gradually reaches constant. The ratio of Q^4 (−111 ppm)/Q^3(−102 ppm) was, however, found to be nearly 2.0 regardless of reaction time, which is consistent with the micropore formation illustrated in Figure 9c,d.

Figure 9c,d respectively indicate that the micropores around 1 nm in size are formed continuously and are stable and that the condensation of silanol groups created in the pores causes enlargement of the pores. From this model, point Q in Figure 6 and point P in Figure 5 are thought to be consistent with the transition point from Figure 9c to Figure 9d.

Finally, it would be of interest to calculate S_{int} which could be expected by the micropore formation model. The superlattice repeat (H in Figure 9a) has been known to be ranged from 1.8 to over 11 nm, but mostly between 2.55 and 5.1 nm.[21] By assuming the value of 4.33 nm of which is the same as that of Kunze's specimen, lattice parameters a, b, and c are 4.33, 0.923, and 0.727 nm, respectively, which leads to 17 SiO_4 tetrahedra and 16 MgO_6 octahedra in the full wave.[21] In stage (c) in Figure 9, the micropores, each of which has free dimensions of ca. 4.4 × 1 × 0.92 nm, are filled with nitrogen molecules. Since the diameter of nitrogen is about 0.4 nm and the actual weight in grams of an atom is atomic weight × 1.6602×10^{-24}, S_{int} is calculated to be about 450 m^2/g. This value is a definite so long as the unit silicate layer consists of three Si_2O_5 sheets as shown in Figure 9c, and the pore size could be more than 0.8 nm. If silanol groups created in the pores is not condensed at all, the layer structure, corresponding to stage (d), with six

(20) Liebau, F. *Structural Chemistry of Silicates*; Springer-Verlag: Berlin, 1985; pp 212−229.
(21) Brindley, G. W.; Brown, G. *Crystal Structures of Clay Minerals and Their X-ray Identification*; Mineralogical Society: London, 1980; pp 2−28.
(22) Engelhardt, G.; Michel, D. *High-Resolution Solid-State NMR of Silicates and Zeolites*; J. Wiley: Chichester, 1987; pp 110−134.
(23) Kirkpatrick, R. J.; Smith, K. A.; Schramm, S.; Turner, G.; Yang,W.-H. *Annu. Rev. Earth Planet. Sci.* **1985**, *13*, 29−35.

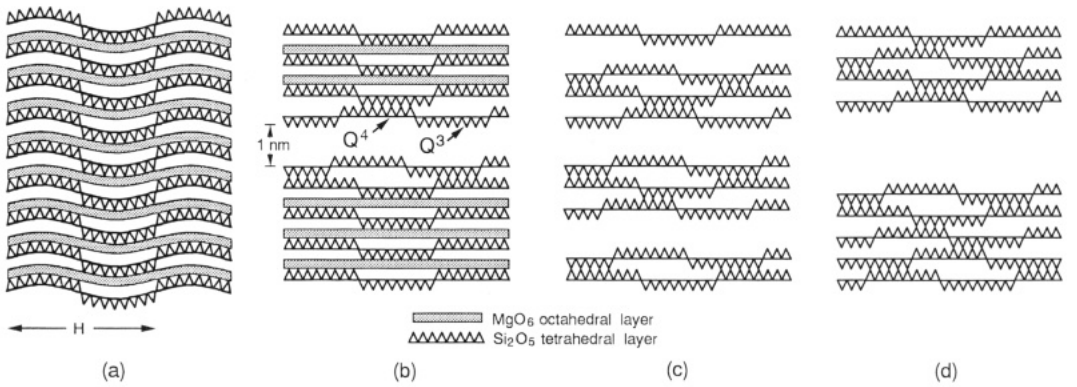

Figure 9. Schematic model of possible micropore formation process: (a) the (001) projection of antigorite, (b) and (c) the micropore created between the layers by sliding and subsequent direct interconnection of the Si_2O_5 layers, and (d) the enlargement of the pore with increasing degree of condensation of silanol groups created in the pores. H indicates the length of superlattice repeat. A and B represent the structural parts giving the ^{29}Si MAS NMR spectrum at −102 ppm for Q^3 and −111 ppm for Q^4 as shown in Figure 8.

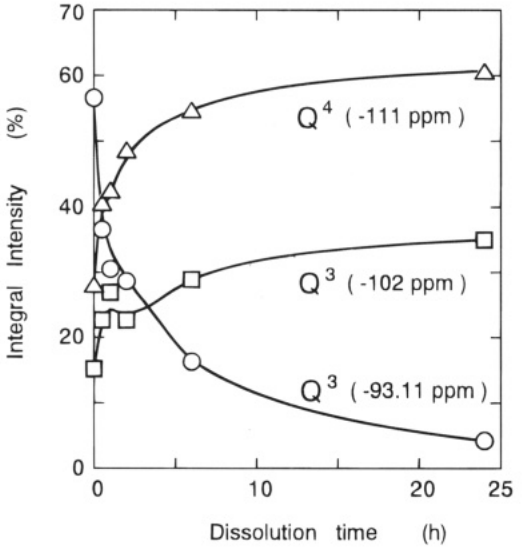

Figure 10. Time dependence of the relative amounts of characteristic structural units of antigorite in the course of acid treatment.

Si_2O_5 sheets in unit layer and interlayer distance of 2 nm has S_{int} of 225 m^2/g. All value of S_{int} obtained in this work is less than 450 m^2/g. However, the values are almost more than 225 m^2/g even when the silanol groups were allowed to be condensed between the layers as shown in Table 1. Consequently, it is assumed from this calculation that the transformation of the stage from (c) to (d) caused on the condensation of silanol groups is really complicated and that the unit silicate layers with three and six Si_2O_5 sheets might be coexist and stack irregularly.

Conclusions

Acid leaching of antigorite ($Mg_3Si_2O_5(OH)_4$) resulted in formation of microporous materials in which pores with sizes of around 1 nm were created upon Mg^{2+} dissolution from the framework. Depending on the conditions of the dissolution and on the rate of silanol group condensation during the dissolution, products with various values of microporous parameters, such as S_{BET}, S_{int}, V, and $2t$, were obtained. The maximum specific surface area and pore volume of the solid containing 2% MgO were about 400 m^2/g and 0.22 mL/g, respectively. Mg^{2+} dissolution eventually resulted in formation of an amorphous silica with more than 99.3% SiO_2 content, of which the specific surface area and pore volume were 170 m^2/g and 0.08 mL/g, respectively. A micropore formation mechanism was proposed based on the results obtained using various analytical methods, and it was shown that the strain occurring due to the misfit between two layers of the composite, the Si_2O_5 sheet, and MgO_6 sheet, decreases with increasing degree of Mg^{2+} dissolution.

Acknowledgment. The authors are grateful to Mr. H. Noma of Kyushu National Industrial Research Institute for obtaining the NMR spectra and his invaluable discussions.

CM950264Y